EXPERIMENTAL VALIDATION AND APPLICATIONS OF A FLUID INFILTRATION MODEL

By Cindy S. Kao[1] and James R. Hunt[2]

ABSTRACT: Horizontal infiltration experiments were performed to validate a plug flow model that minimizes the number of parameters that must be measured. Water and silicone oil at three different viscosities were infiltrated into glass beads, desert alluvium, and silica powder. Experiments were also performed with negative inlet heads on air-dried silica powder, and with water and oil infiltrating into initially water moist silica powder. Comparisons between the data and model were favorable in most cases, with predictions usually within 40% of the measured data. The model is extended to a line source and small areal source at the ground surface to analytically predict the shape of two-dimensional wetting fronts. Furthermore, a plug flow model for constant flux infiltration agrees well with field data and suggests that the proposed model for a constant-head boundary condition can be effectively used to predict wetting front movement at heterogeneous field sites if averaged parameter values are used.

INTRODUCTION

Soil and aquifers have been polluted by the release of contaminated water and non-aqueous-phase liquids at or near the soil surface. The migration of these liquids through the vadose zone is largely controlled by gravitational and capillary forces. During near-surface spills, water and non-aqueous-phase liquids act as wetting fluids and are emplaced in fine-grained material due to horizontal spreading by capillary forces and vertical migration by gravity and capillarity. Efforts at site remediation require predictive tools that can delimit the vertical and horizontal spread of a fluid in order to assess the contaminated volume requiring treatment or better characterization. An analytic infiltration model is verified through laboratory experiments and applications are demonstrated.

Water movement in the vadose zone has been extensively studied for over 100 years due to its importance in groundwater recharge and agricultural management (Hillel 1980). More recently, considerable effort has been devoted to multidimensional numerical models to predict the movement of water and non-aqueous-phase liquids following release and during remediation. These efforts are supported by well-known physical principles of multiphase flow in porous media, but are limited by extensive parameterization and computational complexity. For many sites of near-surface contamination, such modeling efforts cannot be justified given the limited data on release history, inadequate subsurface characterization, and lack of time. Simpler tools are needed by the profession to direct effort at solving these problems rather than engaging in overanalysis.

Kao and Hunt (1996) presented a model for wetting front migration in porous media that provides a simplification on earlier models and was tested with data published in the literature. The approach was to recognize that infiltration is driven by capillary and gravitational forces but hindered by fluid viscosity. Through analogy with flow in a capillary tube, horizontal wetting front lengths were predicted to propagate as the square root of time as

$$x_f = B\left(\frac{\sigma}{\mu}\right)^{1/2} k^{1/4} t^{1/2} \tag{1}$$

where x_f = distance from the source to the wetting front; σ = fluid-air interfacial tension; μ = fluid viscosity; k = porous media permeability; t = time since release began; and B = a dimensionless geometric factor determined to be 0.5 based on data published in the literature for a range in soil properties and for water and alcohol infiltration. The expression is a simplification of a model originally presented by Green and Ampt (1911), but it is unique in that it explicitly captures dependencies on fluid and media properties. The square root of time dependency of wetting liquids was investigated by Amoozegar et al. (1986), who showed that wetting fronts did move proportionally to the square root of time during horizontal infiltration of toluene, xylene, kerosene, acetone, isopropyl alcohol, and ethylene glycol into five different soils. However they were unable to quantify a relationship between the liquid and soil properties that would enable prediction of wetting front movement.

The model in (1), which was derived for the case of horizontal infiltration into an initially dry soil under an inlet head corresponding to atmospheric pressure, was extended by Kao and Hunt (1996) to consider the effect of initial moisture, S_i, as well as the effect of a negative inlet head, h_0. In the model's most general form, it takes on the form of

$$x_f = \frac{B}{(1 - S_i)^{3/4}}\left(\frac{1}{S_w}\right)^{1/4}\left(\frac{h_f - h_0}{h_f}\right)^{1/2}\left(\frac{\sigma}{\mu}\right)^{1/2}(kk_r)^{1/4}t^{1/2} \tag{2}$$

$$h_f = -\frac{\sigma B^2 \Delta\theta}{2\rho g(S_w k k_r)^{1/2}(1 - S_i)^{3/2}} \tag{3}$$

where h_f = wetting front suction head; S_w = saturation in the wetted region corresponding to the inlet head, h_0; $\Delta\theta$ = difference in moisture content between the wetted and dry regions; k_r = relative permeability; ρ = liquid density; and g = gravitational acceleration.

This paper presents experimental data that tests the range of applicability of (1) along with extensions for partially wet media and the simultaneous presence of water and a non-aqueous-phase liquid. The verified model is then extended to consider two-dimensional flow where analytical expressions provide quantitative estimates of fluid propagation. While the analysis is not exact, the comparison of model predictions with laboratory and field data provides an approximate tool with known uncertainties. The model has applicability to long-term releases of fluids and not for oscillatory introductions of water as is encountered during irrigated agriculture.

[1]Asst. Civ. Engr., Santa Clara Water District, 5750 Almaden Expwy., San Jose, CA 95118-3686. E-mail: cindkao@scvwd.dst.ca.us

[2]Prof., Dept. of Civ. and Envir. Engrg., Univ. of California at Berkeley, Berkeley, CA 94720-1710. E-mail: hunt@ce.berkeley.edu

Note. Associate Editor: Hilary Inyang. Discussion open until July 1, 2001. To extend the closing date one month, a written request must be filed with the ASCE Manager of Journals. The manuscript for this paper was submitted for review and possible publication on March 11, 1999. This paper is part of the ***Journal of Environmental Engineering***, Vol. 127, No. 2, February, 2001. ©ASCE, ISSN 0733-9372/01/0002-0162–0169/$8.00 + $.50 per page. Paper No. 20453.

EXPERIMENTAL METHODS

Experiments were designed to test model predictions in (1) and (2) by investigating a range of soil permeabilities, fluid viscosities, to some extent air-liquid interfacial tension, inlet heads, and initial water saturation. The soils tested varied over four orders of magnitude in permeability, and liquid viscosities, which have not been seriously examined in previous infiltration studies, varied over two orders of magnitude.

The liquids and porous media used in the experiments are described in Tables 1 and 2. The infiltrating liquids were salt solutions (consisting of 0.02 g/L or 0.1 g/L of sodium chloride or 0.1 g/L of sodium fluorescein in deionized water), de-aired tap water, and silicone oil at kinematic viscosities of 1 cs, 50 cs, and 100 cs (1 cs = 1×10^{-6} m^2/s). The silicone oil was used as obtained from the distributor (K. R. Anderson Co., Inc.). A ring tensiometer (Fisher Scientific Surface Tensiomat, Model 21) was used to measure interfacial tensions.

Three porous media were used: 0.35–0.42 mm diameter soda lime glass beads; 2–40 μm silicon dioxide powder; and tuffaceous desert alluvium. The glass beads were purchased from Cataphote, Inc. and were prepared by first soaking and washing them in tap water and laboratory detergent and then rinsing with deionized water until the electrical conductivity of the water-bead mix was consistently small. They were then dried at 105°C overnight. The silicon dioxide powder, which will be referred to as silica powder, is a clean, well-graded silt obtained from Fisher Scientific, Inc. It is similar in appearance to white flour. The silica powder was cleaned and purified by the distributor and was used as purchased. The desert alluvium was obtained from a depth of 0.45 to 0.6 m in Frenchman Flat of the Nevada Test Site. It contains particle sizes ranging from gravel to clay, but only the size fraction smaller than 0.59 mm was used in the laboratory experiments without further alteration. The alluvium is a light brown or tan color. Kao (1996) provides grain size distributions for the silica powder and the alluvium.

The columns were extruded acrylic tubes 1.67 cm in diameter and varied from 35 to 55 cm in length. The bulk densities of the packed soil columns are given in Table 2. The acrylic tubes were hydrophobic. A clear acrylic cap with a small flood chamber that could be vented to the atmosphere was fitted to the inlet of the column, and a rubber stopper with a hole drilled through its center was inserted into the other end. Wire mesh screens separated the porous media from the cap and stopper to prevent the porous media from spilling through the apertures. The size of the mesh openings was not measured, but they were chosen to be small enough to retain the soil particles but large enough to allow free passage of liquid.

TABLE 1. Liquids Media Used in Experiments (Properties Measured at 25°C)

Liquid (1)	ρ (kg/m^3) (2)	μ (10^{-4} Ns/m^2) (3)	σ (N/m) (4)
Water (salt solutions and de-aired tap water)	997	8.9	0.069
Silica oil (1 cs)	814	8.1	0.017
Silica oil (50 cs)	957	479	0.020
Silica oil (100 cs)	961	961	0.020

TABLE 2. Porous Media Used in Experiments

Solid (1)	Air-dry water content (g/g) (2)	Dry bulk density (kg/m^3) (3)	Approximate k (m^2) (4)
Silica powder	6×10^{-4}	1390	10^{-14}
Desert alluvium	0.02	1380	10^{-12}
0.35–0.42 glass beads	2×10^{-4}	1400	10^{-10}

Water saturation was monitored in experiments performed on initially water-moistened porous media using eight pairs of electrical resistivity probes located at 5-cm intervals along the column length. The resulting voltage readings were sensitive to small changes in moisture content and were calibrated by measuring the voltage readings corresponding to samples packed to a known density and saturation (Kao 1996).

The experimental procedure consisted of manually packing the porous media into the column to obtain a known bulk density, waiting at least 12 h for columns with initial water present, measuring the permeability to air of the packed column, initiating infiltration, and then tracking the location of the wetting front either visually or with resistivity measurements. A mariotte vessel consisting of a graduated cylinder and a capillary tube was used as the constant-head source. The column was clamped horizontally at a height that yielded the desired inlet head, and the volume of liquid infiltrated with time was measured either by estimating the change in the level of the liquid in the reservoir, or by continuously weighing the reservoir during the infiltration process. The experimental setup was similar to that of Bruce and Klute (1956).

The experiments using negative source pressures were performed at inlet heads of −30 cm, −60 cm, −100 cm, and −150 cm on silica powder only. A solution of 0.1 g/L sodium chloride was infiltrated at inlet heads of −30 cm and −60 cm, and de-aired tap water was used at inlet heads of −100 cm, and −150 cm to reduce formation of air bubbles. In all the experiments, the source pressure was less negative than the bubbling pressure of the silica powder, as determined by manually lowering the source reservoir more than 150 cm below the horizontal soil column and observing that the hydraulic connection between the soil and reservoir remained intact. However, the actual value of the bubbling pressure was not determined due to physical and equipment restraints. A stable hydraulic connection at the column inlet was difficult to obtain during initiation of infiltration at source pressures of −60 cm and lower because of the formation of air bubbles (Kao 1996). Experiments with air bubbles blocking the inlet flood chamber were discontinued and not reported.

The infiltration experiments of water into initially water-moist porous media were performed by infiltrating a 0.1 g/L sodium fluorescein solution into silica powder initially moistened with 0.1 g/L NaCl solution. Experiments were run at initial saturations of 19% and 38%. The movement of the fluorescein solution was recorded by shining a fiber-optic light source upon the column, causing the portion of the column saturated with fluorescein solution to fluoresce, and visually measuring the length of the fluorescent region. The movement of the wetting front, which preceded the fluorescein front substantially, was measured by periodically recording the resistivities at the probes.

The infiltration experiments of silicone oil into porous media initially water-moistened to 19% and 38% saturation were performed by dying 1 cs silicone oil with Automate Red B, a xylene-based dye, and visually tracking the movement of the dyed oil. Water movement was monitored by recording the resistivities at the probes. All experiments were performed in a room that usually varied in temperature by less than 1°C, although on a few occasions temperatures changed by up to 5°C.

Moisture profiles were measured at the end of several experiments in which water or 1 cs silicone oil was infiltrated into initially water-moist powder. Soil samples were scraped out of the column in 1.5–3 cm intervals and the total liquid saturation of each was determined by weighing before and

after drying at 120°C. That temperature was sufficient to volatilize the oil as well as the water.

RESULTS

Fig. 1 compares the measured wetting front propagation with model predictions for infiltration of water into initially air-dried media. Model predictions were based on (1) using a value of 0.5 for the parameter B, as was determined in the earlier analysis of literature data (Kao and Hunt 1996), and the measured value of permeability for each soil.

A second series of experiments was performed using silicone oil at three different viscosities. The measured and predicted results for infiltration into glass beads are shown in Fig. 2. For each viscosity, data were obtained from two or three experimental runs. Similar comparisons are shown in Figs. 3 and 4 for silicone oil infiltration into desert alluvium and silica powder. During infiltration of both water and oil into silica powder or desert alluvium, wetting fronts were distinct and vertical, as expected. However, all wetting fronts in glass beads were not vertical but instead sloped severely at 70–80 degrees from vertical. In these cases, the wetting-front location was taken as the point along the sloped interface that intersected the centerline of the column.

A linear relationship existed between volume infiltrated and wetted length for all cases, and the average value of saturation behind the wetting front was calculated by dividing the volume infiltrated with the total pore volume of the wetted region using values of dry bulk density and grain density. The analysis indicated that the saturation in the wetted region was 75% for glass beads and about 60% for desert soil and silica powder. The saturation values for desert alluvium and silica powder were lower than values reported in the literature. For instance, Bruce and Klute (1956) reported saturation values ranging from 70 to 90% during horizontal infiltration into glass beads and sand, while Nielsen et al. (1962) reported saturation values close to 100% during horizontal infiltration into Columbia silt loam. The lower saturations in the current investigation may be attributed to the fine particle size of the silica powder (2–40 μm) and the wide range of particle sizes for the desert alluvium (0.5–590 μm); however, a definitive explanation is not available.

Infiltration of water under negative inlet heads was performed on initially air dried silica powder, and the results are compared with predictions from (2) and (3). The glass beads and desert alluvium were not used because of difficulties in initiating infiltration into these soils at low inlet heads. Wetting front movement under −30 cm and −60 cm inlet heads was similar to movement under zero inlet head and agrees well with predictions, as shown in Fig. 5(a). At inlet heads of −100 cm and −150 cm, however, the wetting front traveled more quickly than predicted in some cases, while movement was severely inhibited in other cases, as illustrated in Fig. 5(b). An analysis of the volume of liquid infiltrated under zero and negative inlet heads indicates that the saturation in the wetted region was nearly the same in all cases. This further supports the condition that inlet heads were less negative than the bubbling pressure head of the powder.

The location of the wetting front during water infiltration into initially water-moist silica powder is plotted in Fig. 6 and

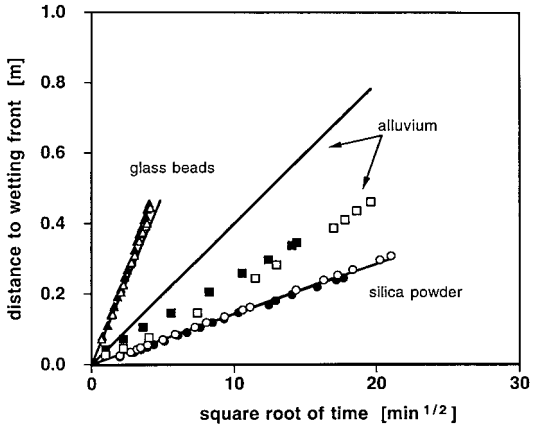

FIG. 1. Data (Symbols) and Model Predictions (Lines) for Infiltration of Water into Initially Air-Dried Porous Media (Inlet Heads Were 0 cm, Opened and Closed Symbols Represent Duplicate Experiments)

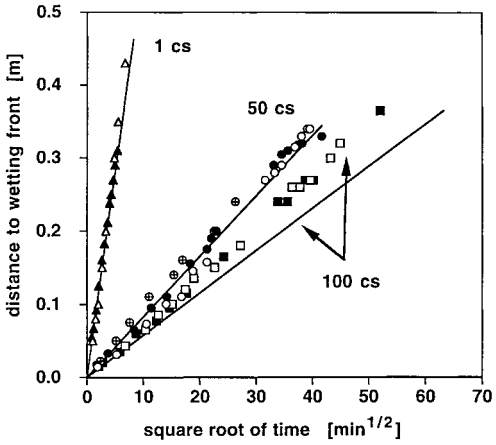

FIG. 2. Data (Symbols) and Model Predictions (Lines) for Infiltration of Silicone Oil into Glass Beads (Inlet Heads Were 0 cm)

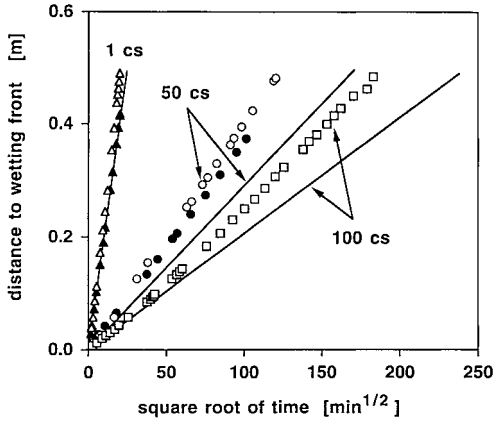

FIG. 3. Data (Symbols) and Model Predictions (Lines) for Infiltration of Silicone Oil into Desert Alluvium (Inlet Heads Were 0 cm)

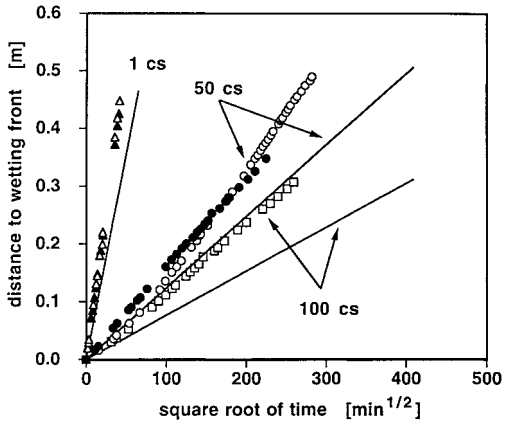

FIG. 4. Data (Symbols) and Model Predictions (Lines) for Infiltration of Silicone Oil into Silica Powder (Inlet Heads Were 0 cm)

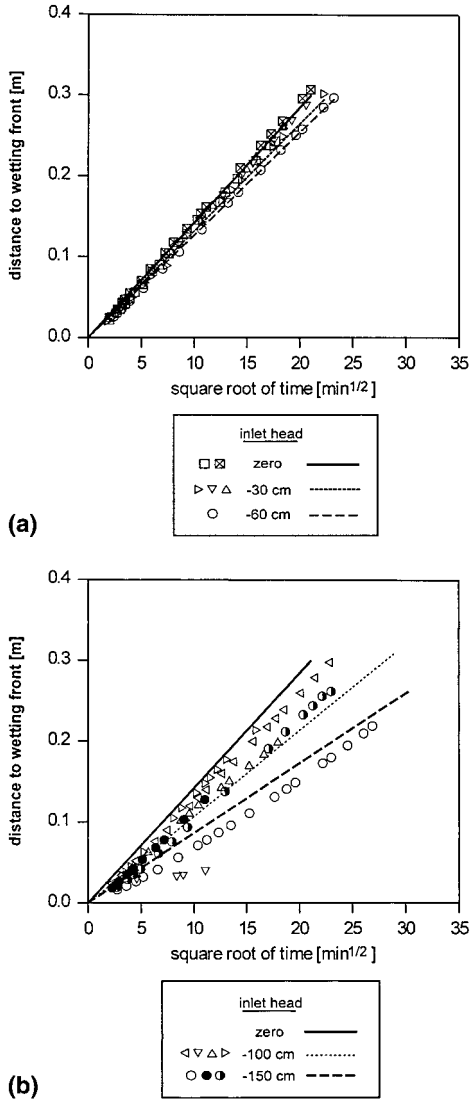

FIG. 5. Data (Symbols) and Model Predictions (Lines) for Water Infiltration into Initially Air-Dried Silica Powder: (a) at Inlet Heads of Zero (Squares), −30 cm (Triangles), and −60 cm (Circle); (b) at Inlet Heads of −100 cm (Triangles) and −150 cm (Circles) (Predicted Infiltration at an Inlet Head of Zero Is Added for Comparison)

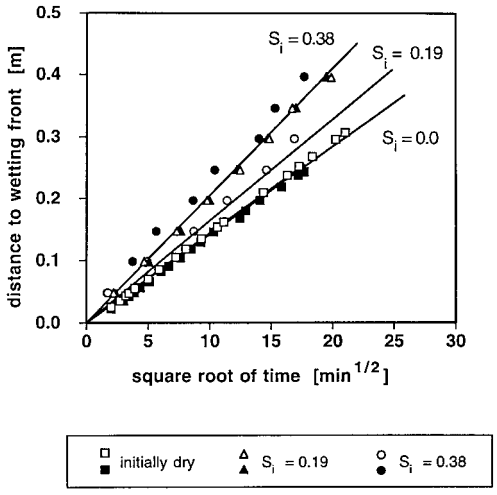

FIG. 6. Data (Symbols) and Predictions (Lines) for Wetting Front Movement during Infiltration of Water into Initially Water-Moist Powder (Opened and Closed Symbols Represent Duplicate Experiments)

compared with predictions from (2) and (3). The infiltrating water contained 0.1 g/L sodium fluorescein and the silica powder was initially moistened with a 0.1 g/L solution of NaCl to saturations of 19% and 38%. The wetting-front location was easily identified for the cases of 19% initial moisture content because of the steep drop in resistivity values upon arrival of the wetting front. Identification of wetting-front arrival for initial saturations of 38% was more difficult because the drop in voltage readings was more gradual. In these cases, the point on a voltage-time curve corresponding to maximum curvature was visually estimated and taken to correspond to the arrival of the wetting front at that probe location. Saturation profiles were measured at the end of an infiltration experiment for each initial saturation level, and they resembled plug flow profiles with a saturation in the wetted region of about 0.65.

Silicone oil (1 cs) was filtrated into silica powder moistened to 19% and 38% initial water saturations. The experiments were run under zero source pressure. The distance to the oil front was plotted against the square root of time and compared

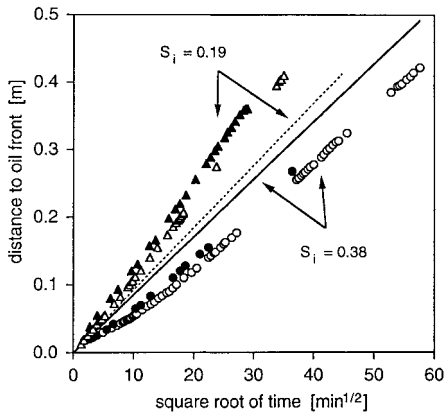

FIG. 7. Data (Symbols) and Model Predictions (Lines) for Infiltration of 1 cs Silicone Oil into Initially Water-Moist Silica Powder (Opened and Closed Symbols Represent Duplicate Experiments)

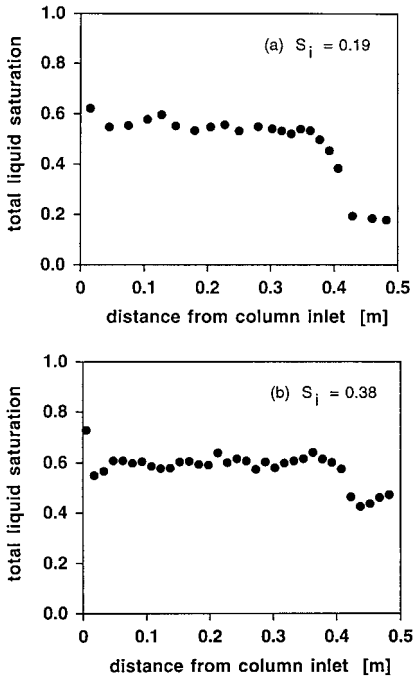

FIG. 8. Total Liquid Saturation for Infiltration of 1 cs Silicone Oil into Initially Water-Moist Silica Powder: (a) After 20.5 h of Infiltration with Initial Water Saturation of 0.19; (b) After 55 h of Infiltration with Initial Water Saturation of 0.38

with model predictions from (3), assuming that the initial water was immobile. The permeability to air of the water-moistened soil column was measured prior to infiltration of oil, and this value was used in the predictions. The comparisons are shown in Fig. 7. Electrical resistivity measurements indicate that the water saturation at each probe increased by less than 5% as the oil front approached and then decreased to a saturation slightly less than the initial saturation after the oil reached the probe location, suggesting that the oil displaced a small portion of the initial water through viscous forces (Kao 1996). The water movement was slight enough that the plug flow profile predicted by the model was maintained, as shown in Figs. 8(a and b). However, the total saturation ahead of the measured wetting front is greater than the initial value of 38% in Fig. 8(b).

DISCUSSION

In general, the model predictions compare favorably with experimental results. Fig. 1, which compares results for the case of water infiltration into initially dry media, illustrates the ability of the model to capture large variabilities in hydraulic conductivity. The agreement between the predictions and experimental results also supports the assignment of a value of 0.5 to the constant *B*, as suggested in Kao and Hunt (1996). Model predictions are highly accurate for the two ideal soils, represented by silica powder and glass beads. A larger discrepancy, which cannot yet be explained, exists in the case of infiltration into alluvium. However, even in this case, an inspection of Fig. 1 indicates that the predicted wetting-front lengths exceed the measured values by 80%. This is a reasonable discrepancy given that the alluvium is a real soil and is therefore not ideal, unlike the controlled manufacture of the glass beads and silica powder.

In addition to capturing the effects of different permeabilities, the model also successfully represents the effects of viscosity and interfacial tension, as shown in Figs. 2–4. Some variability of the predictions from the data is evident, particularly for infiltration of oil into silica powder, but the discrepancies are less than 40% of experimental values.

When inlet heads were lowered below a value of zero, representing a suction effect, little effect was experimentally observed at low suctions. The expectation is that the model will work well at inlet heads between zero and the bubbling pressure head because the wetted region should be close to liquid saturation. When the inlet head is more negative, errors are expected to increase because air bubbles will block liquid movement and reduce the liquid permeability behind the wetting front. The comparisons shown in Figs. 5(a and b) show little observed experimental effect for inlet beads of -60 cm or greater; predictions are highly accurate at these inlet heads as well. At inlet heads of -100 cm and -150 cm, variability among replicates preclude an assessment of the predictive capacity of the model. The experimental data does indicate that wetting-front propagation is retarded at inlet heads more negative than -100 cm. However, spills of contaminated water and non-aqueous-phase liquids with significantly negative inlet heads are rare in the subsurface.

Figs. 1–5 compare predictions with data for infiltration of water and oil into initially air-dry porous media. Figs. 6 and 7 show similar comparisons for infiltration of water and oil, respectively, into initially water-moist porous media. Model predictions in Fig. 6 capture the general behavior of the measured data for infiltration of water into initially water-moist soil. However, variations in column packing likely resulted in inconsistencies in data reproducibility, as illustrated by the 30% discrepancy in measured wetting-front lengths for duplicate columns packed to 38% initial water saturation. Therefore, differences between predictions and data are caused by both model approximations and sensitivity to experimental methods. Fig. 6 shows that the effect of initial water saturation on wetting-front propagation during water infiltration is moderate.

Model predictions of oil infiltration into water moist soil tend to be less accurate than in the case of water infiltration. As shown in Fig. 7, the model underpredicts the location of the oil front for the case of 19% initial saturation while overpredicting oil-front movement for the case of 38% initial water saturation. Errors between predicted oil-front locations and measured locations are less than 30%. Errors may result from the lubricating effects of the water coating the grains, which is not taken into account by the model, and by the model assumption that initial saturation is spatially nonvarying at the pore scale, while in reality smaller pores are more highly saturated than larger pores. It should be noted that the front propagation at 19% initial water saturation was approximately equal to 1 cs oil infiltration into initially dry silica powder. This could possibly be a lubrication effect or enhanced migration caused by the positive spreading coefficient for the oil-water-air system. At high initial saturations, small saturated pores block movement of the oil phase, effectively increasing the tortuosity of pathways available for oil movement.

Overall, the experimental results are generally well predicted by the model for infiltration of both water and oil into both air-dried and initially water-moist porous media. The results support the following conclusions:

- Movement of the wetting front during horizontal infiltration is dependent upon the product of $k^{1/4}$ and $(\sigma/\mu)^{1/2}$.
- The effects of negative inlet heads and initial water saturation on propagation of the wetting front are relatively minor.
- Model predictions of wetting front location are usually within 40% of experimental data.

APPLICATIONS

The following sections describe applications of the model to multidimensional infiltration from small area sources. The use of a plug flow model in predicting constant flux infiltration is also discussed, and predictions are compared with measured data reported in the literature.

Multidimensional Infiltration

The theory of Green and Ampt (1911) can be used to predict vertical infiltration using their classic equation

$$t = \frac{\Delta\theta\mu}{\rho g k k_r}\left[z_f + h_f \ln\left(1 - \frac{z_f}{h_f}\right)\right] \tag{4}$$

where z_f = depth to the wetting front (a positive value). For infiltration under zero or positive source pressures, k_r, may be approximated with a value of one (i.e., soil is assumed completely saturated). When $z_f \ll -h_f$ capillary forces dominate conversely, when $z_f \gg -h_f$, gravity dominates and the front propagates linearly with time. Kao and Hunt (1996) provided an approximate time for vertical flow to be dominated by gravity given by

$$t_g = \frac{9}{16}\frac{\sigma\mu(\Delta\theta)^2}{\rho^2 g^2 k^{3/2}} \tag{5}$$

For water infiltration into dry soil where $\Delta\theta = 0.35$ and the permeability is 5×10^{-11} m^2, only 2 min is required for gravity to dominate over capillarity.

Many studies have been performed to apply mathematical models to predict infiltration from a line source, often with reference to the common practice of furrow irrigation (Raats

1970; Youngs 1972; Warrick and Lomen 1974; Fok and Chiang 1984; Vogel and Hopmans 1992; Fonteh and Podmore 1993; Waechter and Mandal 1993; Tabuada et al. 1995). The combination of the horizontal and vertical infiltration models in (1) and (4) can be used to estimate the shape of the wetted region below a line source of fluid by assuming horizontal and vertical infiltration are independent of each other. In reality, the horizontal wicking will initially retard the downward movement of water, and vice-versa, because both processes compete for the available liquid, which is limited by the conductivity of the soil. However, in coarse soils such as sands, vertical flow will soon govern as the rate of horizontal expansion decreases and is limited by the decreasing head gradient rather than by the availability of liquid. The analytical models in (1) and (4) also predict the extent of the wetted region at any time t during infiltration from a furrow, but with far less complexity than other approaches.

Fig. 9(a) shows the infiltration profile from a furrow at time t after the initiation of infiltration. A coordinate system is taken such that the origin is at the edge of the furrow, the vertical z-axis is positive downwards, and the horizontal x-axis is positive pointing away from the furrow. The coordinates at any point along the front can be obtained by conceptualizing the flow process as a combination of one-dimensional horizontal and vertical infiltration. For example, point A with coordinates (x_a, z_a) can be obtained by recognizing that the time required for the front to travel vertically downwards from a depth z_a to the maximum depth z_d is equal to the time available for the front to move horizontally from the furrow edge to a distance x_a. The distance x_a is then obtained from

$$x_a = B\left(\frac{\sigma}{\mu}\right)^{1/2} k^{1/4}(t - t_a)^{1/2} \tag{6}$$

The corresponding time t_a is obtained from (4) where z_f is equal to z_a and h_f is obtained from (3). The relative permeability is approximated with the value of one. Using (4) and (6), the profile of the wetting front at any time t can be obtained. Fig. 9(b) is an example of the wetting front evolution predicted from (4) and (6) using parameter values of $\Delta\theta = 0.35$ and $k = 5 \times 10^{-11}$ m^2. The wetted region takes on a tear-shaped profile rather quickly as gravity dominates the vertical flow. Eq. (4) and (6) should provide good predictions in these coarse soils, while in finer-grained material, they would provide an outer bounds for estimating the wetted region during infiltration.

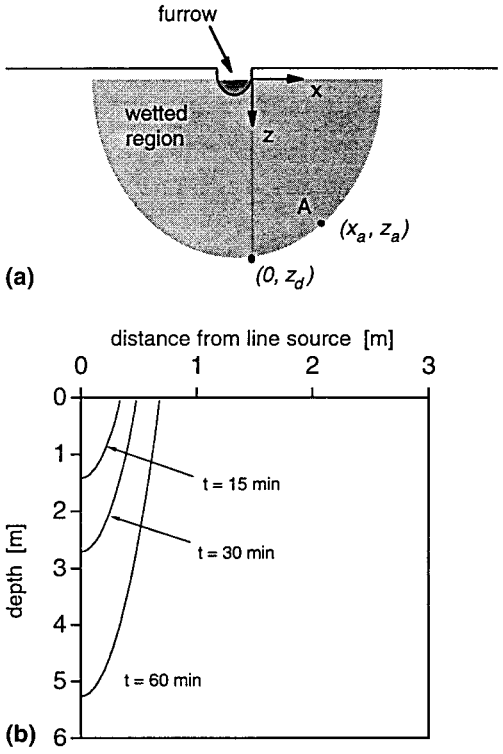

FIG. 9. View of: (a) Wetted Cross Section during Infiltration from a Furrow; (b) Example of Wetting Front Evolution Calculated from Eqs. (4) and (6) (Calculations Assume Change in Moisture Content of 0.35 and Permeability of 5×10^{-11} m^2; Note That Horizontal Scale Is Twice as Large as Vertical Scale)

In addition to a line source, the infiltration models can be used to consider an areal source of fluid in the soil of radius r^*. Vertical migration is caused by capillary and gravitational forces, while horizontal, radial flow is attributed solely to capillary flow. The objective is to determine the approximate shape of the wetted zone beneath such a source by separating vertical flow from horizontal, radial flow.

At some depth z, there is a radial volumetric flow rate per unit depth of $q(t)$ given by

$$q(t) = 2\pi r v(r) \tag{7}$$

where $v(r)$ = fluid velocity. Darcy's law is used for this radial, horizontal velocity at a fixed time t, and the differential equation is integrated from $h = 0$ at $r = r^*$ to $h = h_f$ at $r = R(t)$, where r^* is the radius of the source and $R(t)$ is the radius of the wetted region at that depth. The solution of the differential equation is

$$q(t)\ln\left[\frac{R(t)}{r^*}\right] = -\frac{2\pi\rho g k h_f}{\mu} \tag{8}$$

Since horizontal flow causes the wetted region to enlarge, $q(t)$ and $R(t)$ are related through

$$q(t) = \Delta\theta 2\pi R\frac{dR}{dt} \tag{9}$$

and upon substitution of this expression for $q(t)$ into (8) and integrating over time gives a functional relationship between wetted radius and time

$$t = -\frac{\Delta\theta\mu}{2\rho g k h_f} R^2\left[\ln\frac{R}{r^*} - \frac{1}{2}\left(1 - \frac{r^{*2}}{R^2}\right)\right] \tag{10}$$

recalling that t is positive since h_f is negative.

Fig. 10(a) illustrates the time-distance relationship predicted by (10) for radial infiltration for a typical fine sand having a permeability of 5×10^{-11} m^2 and $\Delta\theta = 0.35$, with $r^* = 0.1$ m. Fig. 10(b) replots the computed data, showing that the wetting front is approximately proportional to the square root of time.

During infiltration from an areal source at the surface, the shape of the wetting front at any time t_d is obtained by treating vertical and radial infiltration as two independent processes, as in the case of infiltration from a line source discussed previously. The maximum depth attained by the wetting front is calculated from Green and Ampt's (1911) vertical infiltration equation, (4), with $t = t_d$, while the radial extent of infiltration at any depth z_a is obtained from (10) with $t = t_d - t_a$, where t_a is the time needed for the wetting front to reach the depth z_a. The results of these calculations for the fine sand modeled in Figs. 10(a and b) are illustrated in Fig. 10(c), which shows the evolution of the wetting front depth as well as radial extent as a function of time.

Constant Flux Vertical Infiltration

A plug flow approach also provides predictions of wetting-front movement during vertical infiltration when a constant flux is imposed over a large areal extent. Long-term fluid re-

lease at a flux of U (m^3/m^2-s) establishes one-dimensional flow in the wetted region at the unsaturated hydraulic conductivity $K(\theta_w)$ which is equal to $\rho g k k_r(\theta_w)/\mu$. The wetting front location, z_f, is then given by

$$z_f = \frac{K(\theta_w)}{\theta_w - \theta_i} t = \frac{U}{\theta_w - \theta_i} t \tag{11}$$

Given the applied flux, U, and the initial moisture content, the only variable that must be determined is θ_w. This moisture content corresponds to an unsaturated hydraulic conductivity equal in value to the applied flux, and so may be obtained from a $K(\theta)$ curve. For moderately permeable soils, gravitational forces rapidly dominate over capillary as indicated in (5). The approximation given by (11) is not new and in fact has been recognized to provide an estimate of wetting front

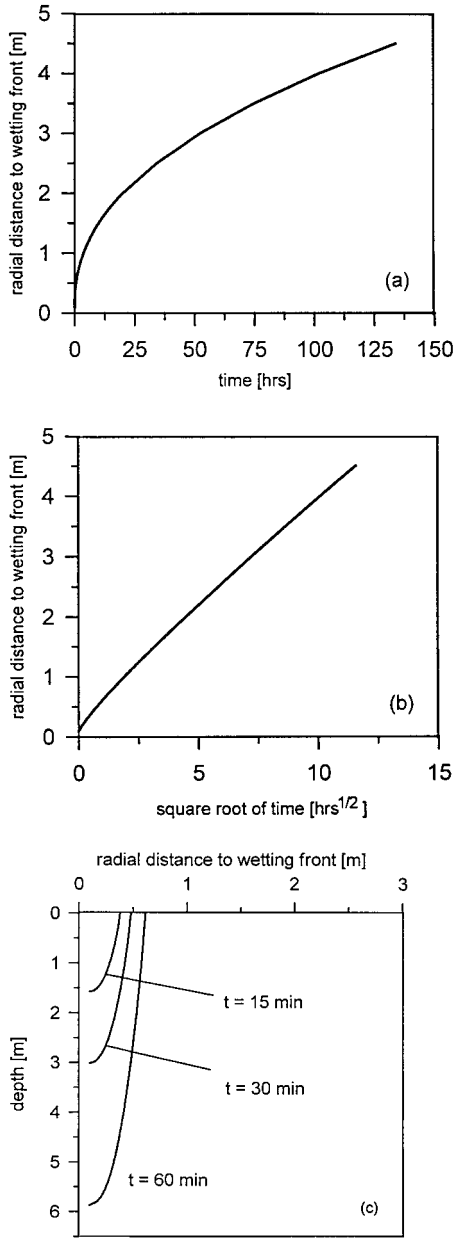

FIG. 10. Examples of Wetting Front Evolution for Areal Source of Water with Radius of 0.1 m (Calculations Assume a Change in Moisture Content of 0.35 and a Permeability of 5×10^{-11} m^2): (a) Radial Distance from Source to Wetting Front as a Function of Time as Predicted by Eq. (10); (b) Showing Radial Distance to Wetting Front Is Approximately Proportional to Square Root of Time; (c) Evolution of Wetting Front in Two Dimensions (Note That Horizontal Scale Is Twice Vertical Scale)

TABLE 3. Parameters Used in Plug Flow Estimations for Constant Flux Infiltration Experiments

Experiment (1)	Flux (m/h) (2)	Average θ_i (3)	Average $\Delta\theta$ (4)	Reference (5)
Las Cruces trench site	0.0182	0.09	0.23	Wierenga et al. (1991)
Alternating layers of sand and loam in lysimeter	0.0204	0.028	0.35	Hills et al. (1989b)

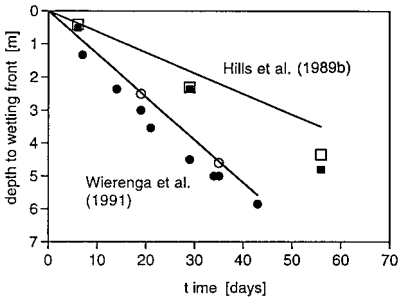

FIG. 11. Comparison between Measured Data (Solid Symbols), Numerical Solutions (Open Symbols), and Plug Flow Model (Lines) [Measured Data and Numerical Solutions Were Reported by Wierenga et al. (1991) (Circles) and Hills et al. (1989b) (Squares)]

movement (Hills et al. 1989a). However, its predictive capabilities have not been fully investigated, while modelers have preferred the challenges of more-sophisticated numerical approaches.

To illustrate the relevance of the simple plug flow approximation, predictions from (11) are compared with data from two studies: infiltration into a 6-m-deep lysimeter packed with alternating layers of sand and loam (Hills et al. 1989b), and infiltration at the heterogeneous Las Cruces trench site located in semi-arid southern New Mexico (Wierenga et al. 1991). In both cases, an average value of θ_w was obtained from preliminary data measured by the investigators to estimate the hydraulic parameters. The parameters used in the predictions are shown in Table 3, and comparisons between the data, numerical predictions of Hills et al. (1989b) and Wierenga et al. (1991), and the plug flow model are shown in Fig. 11. The plug flow model predicts wetting-front movement at the heterogeneous Las Cruces field site as accurately as a finite-difference algorithm, and it compares well with the numerical and measured data in the lysimeter study. The only required measurements are initial moisture contents and moisture contents corresponding to an unsaturated hydraulic conductivity equal to the applied flux. These values can be obtained over a profile and averaged, as was done for the Las Cruces site. In contrast to the simplicity of the solution offered by direct application of (11), traditional mathematical and numerical approaches used to model infiltration into the alternating sand and loam lysimeter presented by Hills et al. (1989b) requires significantly more time and effort, as exemplified in the study performed by Warrick (1991).

SUMMARY

Water and non-aqueous-phase liquid infiltration through near-surface soils is quantified by a model that incorporates a minimal set of fluid and porous media properties. Horizontal infiltration experiments of increasing complexity have verified the model's dependence on medium permeability and fluid viscosity. While interfacial surface tensions were varied, there was not a comprehensive test on its contributions to wetting-front propagation. Fluid infiltration into nearly dry porous me-

dia at near-zero inlet heads is a situation likely encountered at many hazardous-waste sites and model predictions were generally within 40% of experimental observations. Experiments with water infiltration into partially wet porous media showed a slight dependence on initial saturation as expected by the model. Less predictive success was obtained for oil infiltration into partially water-saturated fine media.

The one-dimensional model was extended to predicting vertical and two-dimensional wetting fronts through a reasonable decoupling of vertical, gravity-dominated flow from capillary-driven horizontal flow. The analytical models for the shape of line and areal source wetting fronts had the expected shapes, and predictions were relatively easy to acquire. The one-dimensional vertical infiltration analysis was in good agreement with laboratory and field studies.

The assumption of plug flow in porous media has been successfully applied for more than 100 years and continues to offer a number of advantages. Plug flow of wetting fronts is observed in porous media. The square root of time dependence on front length is well established and the inclusion of measurable media and fluid properties provides predictions without the need for calibration. Numerical modeling of fluid flow in the vadose zone is well developed, but requires extensive characterization of porous media properties that may be feasible in all circumstances. This work has shown that reasonable predictions of fluid infiltration are possible that can delimit the vertical and horizontal spread of fluids and associated contaminants in the vadose zone. Such a model will be useful for initial characterization and screening, and then if justified, more complex analysis may be undertaken.

ACKNOWLEDGMENTS

This work was supported by the Environmental Restoration and Waste Management Fellowship program of the U.S. Department of Energy; the NIEHS Superfund Program, grant 3P42 ES04705-13; and the Los Alamos National Laboratory LACOR Program. The research in this paper was conducted at the University of California at Berkeley.

APPENDIX. REFERENCES

Amoozegar, A., Warrick, A. W., and Fuller, W. H. (1986). ''Movement of selected organic liquids into dry soils.'' *Hazardous Waste and Hazardous Mat.*, 3(1), 29–41.

Bruce, R. R., and Klute, A. (1956). ''The measurement of soil moisture diffusivity.'' *Soil Sci. Soc. Am. Proc.*, 20(4), 458–462.

Fok, Y.-S., and Chiang, S.-H. (1984). ''2-D infiltration equations for furrow irrigation.'' *J. Irrig. and Drain. Engrg.*, ASCE, 110(2), 208–217.

Fonteh, M. F., and Podmore, T. (1993). ''A physically based infiltration model for furrow irrigation.'' *Agric. Water Mgmt.*, 23, 271–284.

Green, W. H., and Ampt, G. A. (1911). ''Studies on soil physics: Part I. The flow of air and water through soils.'' *J. Agric. Sci.*, 4, 1–24.

Hillel, D. (1980). *Applications of soil physics*, Academic, San Diego.

Hills, R. G., Hudson, D. B., Porro, I., and Wierenga, P. J. (1989b). ''Modeling one-dimensional infiltration into very dry soils, 2. Estimation of the soil water parameters and model predictions.'' *Water Resour. Res.*, 25(6), 1271–1282.

Hills, R. G., Porro, I., Hudson, D. B., and Wierenga, P. J. (1989a). ''Modeling one-dimensional infiltration into very dry soils, 1. Model development and evaluation.'' *Water Resour. Res.*, 25(6), 1259–1269.

Kao, C. (1996). ''Analysis and verification of a wetting front model for infiltration into soils.'' PhD dissertation, University of California, Berkeley, Calif.

Kao, C., and Hunt, J. R. (1996). ''Prediction of wetting front movement during infiltration into soils.'' *Water Resour. Res.*, 32(1), 55–64.

Nielsen, D. R., Biggar, J. W., and Davidson, J. M. (1962). ''Experimental consideration of diffusion analysis in unsaturated flow problems.'' *Soil Sci. Soc. of Am. Proc.*, 26(2), 107–111.

Raats, P. A. C. (1970). ''Steady infiltration form line sources and furrows.'' *Soil Sci. Soc. Am. Proc.*, 34(5), 709–714.

Tabuada, M. A., Rego, Z. J. C., Vachaud, G., and Pereira, L. S. (1995). ''Two-dimensional infiltration under furrow irrigation: Modelling, its validation and applications.'' *Agric. Water Mgmt.*, 27, 105–123.

Vogel, T., and Hopmans, J. W. (1992). ''Two-dimensional analysis of furrow infiltration.'' *J. Irrig. and Drain. Engrg.*, ASCE, 118(5), 791–806.

Waechter, R. T., and Mandal, A. C. (1993). ''Steady infiltration from a semicircular cylindrical trench and a hemispherical pond into unsaturated soil.'' *Water Resour. Res.*, 29(2), 457–467.

Warrick, A. (1991). ''Travelling front approximations for infiltration into stratified soils.'' *J. Hydro.*, Amsterdam, 128, 213–222.

Warrick, A., and Lomen, D. (1974). ''Time dependent linearized infiltration: Line sources.'' *Soil Sci. Soc. Am. Proc.*, 38, 568–572.

Wierenga, P. J., Hills, R. G., and Hudson, D. B. (1991). ''The Las Cruces trench site: Characterization, experimental results, and one-dimensional flow predictions.'' *Water Resour. Res.*, 27(10), 2695–2705.

Youngs, E. G. (1972). ''Two and three dimensional infiltration: Seepage from irrigation channels and infiltrometer rings.'' *J. Hydro.*, Amsterdam, 15, 301–315.